

# First-principles theory of cation and intercalation ordering in $\text{Li}_x\text{CoO}_2$ <sup>1</sup>

C. Wolverton, Alex Zunger \*

National Renewable Energy Laboratory, Golden, CO 80401, USA

## Abstract

Several types of cation- and vacancy-ordering are of interest in the  $\text{Li}_x\text{CoO}_2$  battery cathode material since they can have a profound effect on the battery voltage. We present a first-principles theoretical approach which can be used to calculate both cation- and vacancy-ordering patterns at both zero and finite temperatures. This theory also provides quantum-mechanical predictions (i.e., without the use of any experimental input) of battery voltages of both ordered and disordered  $\text{Li}_x\text{CoO}_2/\text{Li}$  cells from the energetics of the Li intercalation reactions. Our calculations allow us to search the entire configurational space to predict the lowest-energy ground-state structures, search for large voltage cathodes, explore metastable low-energy states, and extend our calculations to finite temperatures, thereby searching for order–disorder transitions and states of partial disorder. We present the first prediction of the stable spinel structure  $\text{LiCo}_2\text{O}_4$  for the 50% delithiated  $\text{Li}_{0.5}\text{CoO}_2$ . © 1999 Elsevier Science S.A. All rights reserved.

**Keywords:**  $\text{LiCoO}_2$ ; Ordering; First-principles total energies; Spinel; Li intercalation

## 1. Introduction and methodology

The  $\text{LiMO}_2$  ( $M = 3d$  metal) oxides form a series of structures based on an octahedrally coordinated network with anions (O) on one fluidized catalytic cracking (fcc) sublattice and cations (Li and M) on the other [1]. When Li is de-intercalated from the compound, it creates a vacancy (denoted  $\square$ ) that can be positioned in different lattice locations. Hence, there are three types of ordering problems of interest in these materials (we focus on  $\text{LiCoO}_2$ ): (i) Li/Co ordering in  $\text{LiCoO}_2$  ( $x = 1$ ) leads to ordered  $R\bar{3}m$  at low temperature and disordered Li/Co (rocksalt) at high temperature. (ii) Similarly,  $\square/\text{Co}$  ordering in the completely deintercalated  $\square\text{CoO}_2$  ( $x = 0$ ) is also of interest. (iii) The vacancies left behind by Li extraction can form ordered vacancy compounds in partially deintercalated  $\text{Li}_x\text{CoO}_2$ , leading to a  $\square/\text{Li}$  ordering problem for intermediate compositions  $0 \leq x \leq 1$ . We refer to the first two of these ordering problems as *cation ordering* since they occur at fixed composition (either fully intercalated or

deintercalated) and deal with the positions of the cations. The third type of ordering we call *intercalation ordering* since it deals with a fixed  $\text{CoO}_2$  framework and the ordering may occur upon intercalation or deintercalation of Li as a function of composition. In several recent papers which we review here [2–4], we have described a first-principles theoretical approach to examine the energetics and thermodynamics of both cation and intercalation ordering tendencies in the  $\text{Li}_x\text{CoO}_2$  oxide.

We use a three-step first-principles approach to study ordering. The salient points are described here, and more details of the method may be found in Refs. [2–4].

(1) *Total energy calculations:* We calculate the  $T = 0$  total energy of a set of (not necessarily stable) ordered structures via the full potential, all-electron linearized augmented plane wave method (LAPW) with all atomic positions fully relaxed via quantum mechanical forces. The highly accurate LAPW method is, quite literally, the benchmark against which other first-principles methods are tested. We then map the LAPW energies onto a (2) *Cluster expansion (CE)*. The cluster expansion (CE) technique (see, e.g., Ref. [5]) consists of an Ising-like expression in which each substitutional unit is associated with the site of an ideal lattice, and the ‘spin variable’  $S_i$  is given the value  $+1(-1)$  if an  $A(B)$  atom is assigned to site  $i$ . (Note that in the three ordering problems studied,  $A/B = \text{Li/Co}$ ,

\* Corresponding author. Tel.: +1-303-384-6672; Fax: +1-303-384-6531; E-mail: alex@sst.nrel.gov

<sup>1</sup> Presented at the International Meeting on Li Batteries (IMLB), Edinburgh, July 1998. Proceedings to be published in Journal of Power Sources.

$\square/\text{Co}$ , and  $\square/\text{Li}$ .) The energy of any configuration  $\sigma$  can then be written as:

$$E_{\text{CE}}(\sigma) = \sum_f D_f J_f \bar{\Pi}_f(\sigma), \quad (1)$$

where  $f$  is a figure comprised of several lattice sites (pairs, triplets, etc.),  $D_f$  is the number of figures per lattice site,  $J_f$  is the Ising-like interaction for the figure  $f$ , and  $\bar{\Pi}_f$  is a function defined as a product over the figure  $f$  of the variables  $S_i$ , averaged over all symmetry equivalent figures of lattice sites. We determine  $\{J_f\}$  by fitting  $E_{\text{CE}}(\sigma)$  of  $N_\sigma$  structures to laser Doppler anemometry (LDA) total energies  $E_{\text{LDA}}(\sigma)$ , given the matrices  $\{\bar{\Pi}_f(\sigma)\}$  for these structures. Once the coefficients of the expansion  $\{J_f\}$  are known, the Ising-like expression may be easily evaluated for any substitutional configuration. Thus, one can calculate (via first-principles) the total energy of a few substitutional arrangements, but then effectively search the space of  $2^N$  configurations. Having obtained such a general and computationally simple parameterization of the configuration energy, we subject it to (3) *Monte Carlo simulated annealing*. The third step of our approach involves subjecting the cluster expansion to Monte Carlo simulations so as to investigate the thermodynamic properties of the cation or intercalation ordering.

## 2. Results

We construct separate cluster expansions to describe the different types of structural energetics:

### 2.1. Cation (Li / Co) ordering in $\text{LiCoO}_2$

We have computed formation enthalpies for eight different Li/Co cation arrangements  $\sigma$  of  $\text{LiCoO}_2$  ( $x = 1$ ) on the fcc lattice:

$$\Delta H_f(\sigma, \text{LiCoO}_2) = E_{\text{tot}}(\sigma, \text{LiCoO}_2) - E_{\text{tot}}(\text{LiO}, \text{B1}) - E_{\text{tot}}(\text{CoO}, \text{B1}), \quad (2)$$

where the last two terms refer to LiO and CoO in the NaCl (B1) structure with lattice constants obtained by minimizing the respective total energies with respect to hydrostatic deformation. These cation arrangements included both the commonly observed layered  $\text{LiCoO}_2$  structure (which we designate ‘CuPt’ because the cations, Li and Co, form the CuPt structure) and the cubic structure derivative of spinel (which we refer to as ‘D4’ because there are important distinctions between this phase and the spinel structure—see below) which have been produced by solution growth at  $\sim 400^\circ\text{C}$ . (see, e.g., Refs. [6,7]). We have mapped the formation energies of these eight cation configurations onto a cluster expansion and found [2]: the ‘cubic’  $\text{LiCoO}_2$

D4 structure is only slightly higher in energy (0.01 eV/formula unit) than the ‘layered’ CuPt structure, the latter being the observed phase of  $\text{LiCoO}_2$  grown at high temperature. A Monte Carlo simulation starting at high temperature and slowly cooling down demonstrates that the layered phase is the lowest-energy cation arrangement out of the  $2^N$  possible structures, and hence, is truly the thermodynamic ground state of  $\text{LiCoO}_2$ . Also, the calculations demonstrate that the disordered cation phase (rock-salt) is not stable thermodynamically at any reasonable temperatures, thus demonstrating that the observed rocksalt phase [8] is kinetically stabilized.

### 2.2. Cation ( $\square / \text{Co}$ ) ordering in $\square \text{CoO}_2$

Similarly, a cluster expansion was constructed from eight  $\square/\text{Co}$  cation arrangements  $\sigma$  of the fully delithiated  $\square \text{CoO}_2$  ( $x = 0$ ) on the fcc lattice:

$$\Delta H_f(\sigma, \square \text{CoO}_2) = E_{\text{tot}}(\sigma, \square \text{CoO}_2) + E_{\text{tot}}(\text{Li}, \text{bcc}) - E_{\text{tot}}(\text{LiO}, \text{B1}) - E_{\text{tot}}(\text{CoO}, \text{B1}) \quad (3)$$

where  $E_{\text{tot}}(\text{Li}, \text{bcc})$  is the total energy of Li in the bcc structure with lattice constant obtained from total energy minimization. The separation in energy between ‘layered’ CuPt and ‘cubic’ D4 increases in  $\square \text{CoO}_2$  (0.14 eV/formula unit) as compared to  $\text{LiCoO}_2$ , due to the symmetry of the phases [2]. The CuPt layered structure of  $\square \text{CoO}_2$  is again predicted to be the lowest energy substitutional cation arrangement. However, this structure has an ABC... stacking of the cation planes, and recent electrochemical measurements of Amatucci et al. [9] have succeeded in completely de-intercalating Li from  $\text{LiCoO}_2$ , forming a  $\square \text{CoO}_2$  structure with the stacking of planes in an AAA... arrangement. Consistent with the observations of Amatucci et al. [9], we find that the  $\square \text{CoO}_2$  in the AAA stacking is lower in energy than the ABC stacking by  $\sim 0.05$  eV/formula unit.

### 2.3. Effect of cation ordering on average voltage

For a  $\text{Li}_x \text{CoO}_2/\text{Li}$  cell, the voltage  $V(x)$  as a function of Li composition is given by [10,11] the Li chemical potential difference between cathode ( $\text{Li}_x \text{CoO}_2$ ) and anode (Li metal):

$$-eV(x) = \mu_{\text{Li}}(\text{Li}_x \text{CoO}_2) - \mu_{\text{Li}}(\text{Li metal}). \quad (4)$$

From this expression, it is straightforward to show the following (see, e.g., Refs. [12] or [13]):

$$\begin{aligned} \Delta H_{\text{react}}^\sigma(x_2, x_1) &= -F \int_{x_1}^{x_2} dx V(x) \\ &= -(x_2 - x_1) F \bar{V}(\sigma, x_2, x_1) \end{aligned} \quad (5)$$

where  $F$  is the Faraday constant and the reaction energy of Li intercalation between two Li compositions  $x_1$  and  $x_2$  is given by:

$$\Delta H_{\text{react}}^{\sigma}(x_2, x_1) = E_{\text{tot}}(\text{Li}_{x_2}\text{CoO}_2, \sigma) - E_{\text{tot}}(\text{Li}_{x_1}\text{CoO}_2, \sigma) - (x_2 - x_1)E_{\text{tot}}(\text{Li, bcc}). \quad (6)$$

Therefore, by computing the energetics of Li intercalation in Eq. (6), we ascertain the average battery voltage. The calculated average voltages for all cation arrangements considered are in the  $\sim 4$  V range. In particular, the average voltage for  $\text{LiCoO}_2$  in the layered CuPt structure (3.78 V) is in reasonable agreement with measured values (4.0–4.2 V) [14]. The cluster expansion of voltage can also be used to predict the average voltages of disordered phases. The random-cation rocksalt phase (3.99 V) is predicted to have a higher average voltage than the ordered CuPt phase (3.78 V). The voltages of *partially* long-range ordered CuPt and D4 phases ( $\eta = 0.88$ ) are increased relative to CuPt and D4 by 0.05 and 0.01 V, respectively. The qualitative effect of disordering raises the energy of  $\square\text{CoO}_2$  more than  $\text{LiCoO}_2$ , and thus raises the average voltage.

#### 2.4. Intercalation ordering and voltage profile in layered $\text{Li}_x\text{CoO}_2$

The Li sites in the  $R\bar{3}m$  CuPt (layered) structure form close-packed (111) planes which yield a two-dimensional triangular lattice, and these Li planes are stacked in a rhombohedral fashion (ABC). Thus, the problem of intercalation ordering of Li and Li-vacancy (denoted  $\square$ ) is an ordering problem on the stacked triangular lattice. Total energies were computed for a large number (16) of ordered vacancy compounds constructed by removing Li atoms from the  $\text{LiCoO}_2$  (CuPt) structure:

$$\Delta E_{\text{int}}^{\sigma}(x) = E_{\text{tot}}(\text{Li}_x\text{CoO}_2, \sigma) - xE_{\text{tot}}(\text{LiCoO}_2, \sigma) - (1-x)E_{\text{tot}}(\text{CoO}_2, \sigma)^-. \quad (7)$$

These 16 energies are mapped onto a cluster expansion on the three-dimensional triangular lattice with two-, three-, and four-body interactions.

The chemical potential difference in Eq. (4) defining the voltage may be computed [11] from (grand canonical) Monte Carlo simulations of the  $\text{Li}_x\text{CoO}_2$  cluster expansion. This provides a completely parameter-free, first-principles prediction of the Li intercalation voltage of the  $\text{Li}_x\text{CoO}_2/\text{Li}$  cell as a function of Li content. The predicted intercalation voltage profiles are shown in Fig. 1. Shown are results for the equilibrium voltage profile both at zero temperature and  $T = 300$  K. Also shown is the voltage profile of the metastable random solid solution phase. Two-phase regions, defined in terms of free energies by tie-lines connecting the two phases, correspond to plateaus

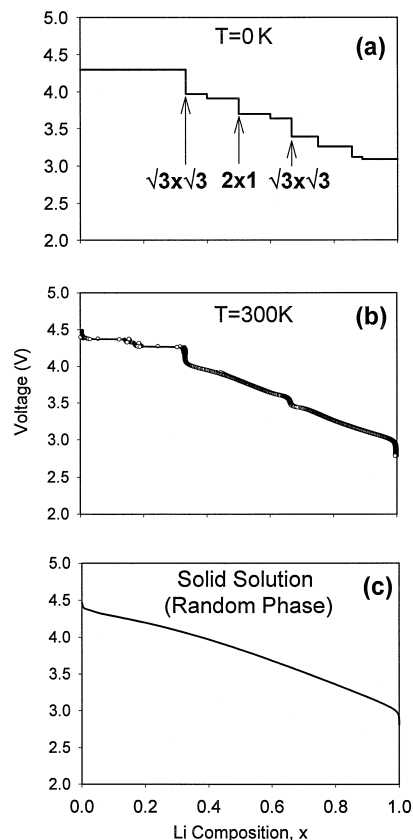


Fig. 1. Predicted Li-intercalation voltage of the  $\text{Li}_x\text{CoO}_2/\text{Li}$  cell as a function of Li composition, calculated from the chemical potential difference in Eq. (4). (a) Equilibrium profile at  $T = 0$  K, calculated analytically from the ordered vacancy formation energies. (b) Equilibrium profile at  $T = 300$  K, calculated from Monte Carlo simulations. (c) Profile of the metastable random solution phase, calculated analytically from the cluster expansion interactions with mean-field ( $T = 300$  K) entropy.

in the voltage profiles. Likewise, the voltage drops are associated with single phase, ordered regions. As the temperature is increased, drops become more rounded and disappear at order–disorder transitions. The voltage profile of the solid solution phase is completely smooth with no discontinuous voltage drops.

Via a combination of Monte Carlo simulations (both grand canonical and canonical), thermodynamic integration, and investigation of finite-size effects, one can map the entire chemical potential–temperature, and hence the voltage–temperature, phase diagram for Li intercalation in  $\text{Li}_x\text{CoO}_2/\text{Li}$  cells. The predicted phase diagram is shown in Fig. 2. Many of the predicted ground state phases undergo order–disorder transitions below room temperature. In equilibrium, three phases are predicted to remain ordered at and above room temperature: the  $2 \times 1$  ( $x = 1/2$ ) and  $\sqrt{3} \times \sqrt{3}$  ( $x = 1/3$  and  $2/3$ ) structures. Reimers et al. [15,16] have observed electrochemically and through X-ray diffraction a monoclinic ordered vacancy compounds at  $x = 1/2$ . Their data suggest a ‘ $2 \times 1$ ’ two-dimensional ordering as we have predicted. Reimers et al.

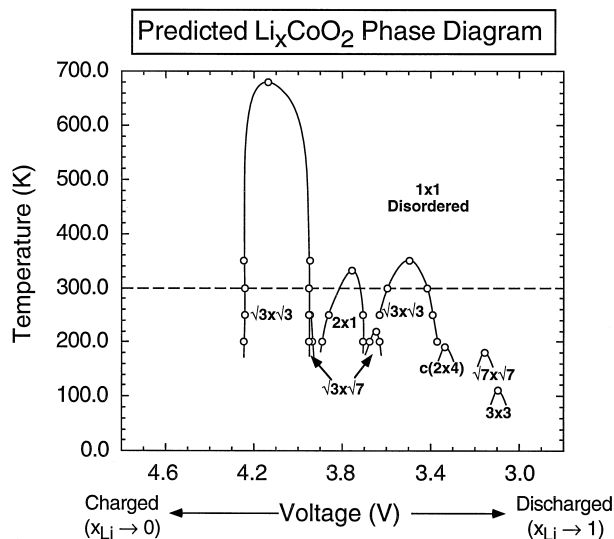


Fig. 2. Predicted  $\text{Li}_x\text{CoO}_2$  voltage–temperature phase diagram. At room temperature (horizontal dashed lined), three vacancy compounds remain ordered.

[15,16] have also measured the order–disorder transition temperature for this phase at  $60^\circ\text{C}$ , and the width of the  $2 \times 1$  phase field at room temperature to be  $\sim 0.1$  V. Our calculations are in excellent agreement with both of these observations. No compounds at  $x = 1/3$  or  $x = 2/3$  have been experimentally reported in  $\text{Li}_x\text{CoO}_2$  (although these  $\sqrt{3} \times \sqrt{3}$  phases have been found in other intercalation compounds). It is possible that the formation of these phases is kinetically inhibited in electrochemical experiments. Also, we have only considered ABC-type stacking sequences in the calculation of this phase diagram, and it is possible that the  $x = 1/3$  phase could disappear from the phase diagram by the emergence of low-energy staged compounds at low-Li content, as has recently been suggested by van der Ven et al. [17]. Additionally, we find no evidence for a two-phase region at high-Li content, as has been observed electrochemically. Future electrochemical experiments to investigate the thermodynamic stability of the predicted ordered vacancy phases would therefore be of great interest.

### 2.5. Intercalation ordering and voltage profile in cubic $\text{Li}_x\text{CoO}_2$

The two ordered forms of  $\text{Li}_x\text{CoO}_2$  which have been synthesized [6,7], ‘layered’ CuPt and ‘cubic’ D4, are extremely similar in terms of atomic coordination sequence: pair and three-body correlations are equivalent, with the first difference between the two occurring at the four-body correlation. Thus, one might expect the two forms of  $\text{Li}_x\text{CoO}_2$  to exhibit similar energies and electrochemical potentials. However, electrochemical properties of the two

compounds are very different: when used as a cathode material in  $\text{Li}_x\text{CoO}_2/\text{Li}$  cells, the cubic D4 structure has a nearly flat voltage plateau at 3.6 V, (for  $1/2 < x \leq 1$ ) which contrasts with the voltage profile of the layered CuPt phase which takes place mostly above 4 V and has several voltage drops and plateaus. We have found [3] that the electrochemical distinction between layered CuPt and cubic D4 is that the intercalation sites for Li of these two compounds changes with Li composition  $x$ : in the cubic phase, Li moves from octahedral ( $O_h$ ) to tetrahedral ( $T_d$ ) sites upon deintercalation, forming a low-energy  $\text{Li}_x\text{CoO}_2$  spinel phase, whereas deintercalation of Li from the layered phase results in formation of ordered vacancy compounds, but Li remains in  $O_h$  sites.

Just as we considered ordered vacancy compounds for the layered phase, we have also computed the total energies of several ‘derivative’ structures  $\text{Li}_x\text{CoO}_2$  formed by partial removal of Li from the cubic structure. We consider both ‘structure preserving’ removal of Li from the parent structures (i.e., removal of Li without changes in the positions of the remaining atoms), as well as ‘symmetry-modifying’ removal of Li (i.e., removal of Li followed by movement of remaining atoms): the energies of these compounds are shown in Fig. 3. We have found that ‘structure preserving’ removal of Li changes the voltages of the CuPt and D4 structures in an almost identical way (due to the similarity of Li/ $\square$  ordering tendencies), and thus, the ‘structure preserving’ removal of Li cannot explain the observed electrochemical differences between CuPt and D4.

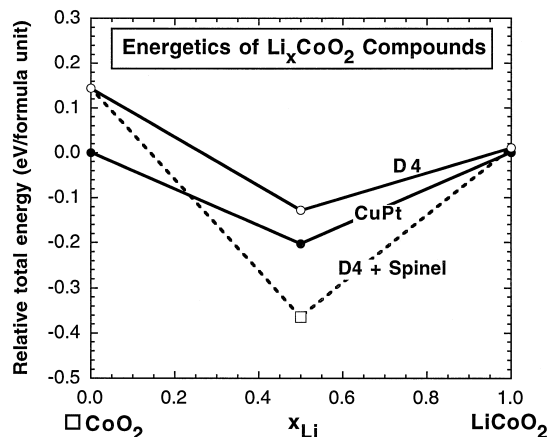


Fig. 3. First-principles calculated energetics of several  $\text{Li}_x\text{CoO}_2$  compounds in the layered and cubic structures. Energies (eV/ $\text{Li}_x\text{CoO}_2$  formula unit) are shown relative to  $x\text{Li}_x\text{CoO}_2 + (1-x)\square\text{CoO}_2$  in the layered structure. The empty (filled) circles connected by solid lines represent the energetics of symmetry-preserving removal of Li from the cubic (layered) structures, respectively. The empty square represents the energy of the  $\text{Li}_x\text{CoO}_2\text{O}_4$  spinel and the dashed lines show the energetic pathway for symmetry-modifying removal of Li from the cubic structure. The average voltages of Eq. (5) are shown graphically as  $3.78\text{V} - m$ , where  $m$  is the slope of the various lines in this figure.

We have found that ‘symmetry modifying’ removal of Li from the cubic phase can account for most of the observed differences between layered and cubic  $\text{Li}_x\text{CoO}_2$ : our results are shown in Fig. 3, where we show that the normal spinel structure has a much lower energy than any of the other compounds calculated at  $x = 1/2$ . While  $x = 1$  D4 has Li and Co in octahedral  $O_h$  positions, the normal spinel structure has two Co in  $O_h$  positions, but Li in tetrahedral  $T_d$  sites. Thus, as Li is deintercalated from the cubic D4 phase, the remaining Li atoms move from  $O_h$  to  $T_d$  sites, as forming a ‘normal’ spinel structure with stoichiometry  $\text{Li}_x\text{CoO}_2\text{O}_4 = 2\text{Li}_{1/2}\text{CoO}_2$ . This calculated  $T_d$  site preference for Li is supported by X-ray diffraction measurements [7].

The low energy of the normal spinel leads (via Eq. (5)) to a significant reduction of the average voltage of the cubic phase from  $x = 1$  to  $x = 1/2$  (3.0 V), as compared to the layered phase (3.4 V), thus explaining the observed difference in voltage between layered and cubic  $\text{Li}_x\text{CoO}_2$  [7,6]. However, although our calculations indicate that the average voltage of the cubic phase is lower than the layered structure down to  $x = 1/2$ , subsequent extraction of Li from the spinel structure corresponds to removal of Li from the (energetically favorable)  $T_d$  sites, and thus costs a large amount of energy. Thus, the average voltage of the cubic structure is predicted to rise sharply (4.8 V) from  $x = 1/2$  to  $x = 0$ . Electrochemical measurements [7,6] of cubic  $\text{Li}_x\text{CoO}_2$  have commonly probed only relatively high Li contents ( $x > 0.5$ ); however, Gummow et al. [7] have observed a sharp increase in voltage (of  $\sim 1$  V) near  $x = 1/2$  in cubic  $\text{Li}_x\text{CoO}_2$ , in agreement with our calculations. If the capacity of Li extraction in the spinel phase  $\text{Li}_x\text{CoO}_2\text{O}_4$  would be improved, our calculations will provide a prediction that this spinel would make a high voltage ( $\sim 4.8$  V) battery cathode.

## Acknowledgements

This work was supported by the Office of Energy Research (OER) [Division of Materials Science of the Office of Basic Energy Sciences (BES)], U.S. Department of Energy, under contract No. DE-AC36-83CH10093.

## References

- [1] T.A. Hewston, B.L. Chamberland, *J. Phys. Chem. Solids* 48 (1987) 97.
- [2] C. Wolverton, A. Zunger, *Phys. Rev. B* 57 (1998) 2242.
- [3] C. Wolverton, A. Zunger, *J. Electrochem. Soc.* 145 (1998) 2424.
- [4] C. Wolverton, A. Zunger, *Phys. Rev. Lett.* 81 (1998) 606.
- [5] A. Zunger, in: P.E.A. Turchi, A. Gonis (Eds.), *Statics and Dynamics of Alloy Phase Transformations*, NATO ASI Series, Plenum, New York, 1994.
- [6] E. Rossen, J.N. Reimers, J.R. Dahn, *Solid State Ionics* 62 (1993) 53.
- [7] R.J. Gummow, D.C. Liles, M.M. Thackeray, *Mater. Res. Bull.* 28 (1993) 235.
- [8] M. Antaya, K. Cearn, J.S. Preston, J.N. Reimers, J.R. Dahn, *J. Appl. Phys.* 76 (1994) 2799.
- [9] G.G. Amatucci, J.M. Tarascon, L.C. Klein, *J. Electrochem. Soc.* 143 (1996) 1114.
- [10] W.R. McKinnon, R.R. Haering, in: R.E. White, J.O’M. Backris, B.E. Conway (Eds.), *Modern Aspects of Electrochemistry*, Vol. 15, Plenum, New York, 1983, p. 235.
- [11] J.N. Reimers, J.R. Dahn, *Phys. Rev. B* 47 (1993) 2995.
- [12] C. Julien, G.-A. Nazri (Eds.), *Solid State Batteries: Materials Design and Optimization*, Chap. 1, Kluwer, Boston, 1994.
- [13] M.K. Aydinol, A.F. Kohan, G. Ceder, K. Cho, J. Joannopoulos, *Phys. Rev. B* 56 (1997) 1354.
- [14] K. Mizushima, P.C. Jones, P.J. Wiseman, J.B. Goodenough, *Mater. Res. Bull.* 15 (1980) 783.
- [15] J.N. Reimers, J.R. Dahn, U. von Sacken, *J. Electrochem. Soc.* 140 (1993) 2752.
- [16] J.N. Reimers, J.R. Dahn, U. von Sacken, *J. Electrochem. Soc.* 139 (1992) 2091.
- [17] A. van der Ven, M.K. Aydinol, G. Ceder, *J. Electrochem. Soc.* 145 (1998) 2149.